# MULTI-ENERGY MICROGRID SCHEDULING: A MULTI-VECTOR DEMONSTRATOR CASE STUDY

Natalia-Maria ZOGRAFOU-BARREDO
Newcastle University – UK
n.zografou-barredo2@newcastle.ac.uk

Charalampos PATSIOS
Newcastle University – UK
haris.patsios@newcastle.ac.uk

Sara Louise WALKER
Newcastle University – UK
sara.walker@newcastle.ac.uk

Peter DAVISON
Newcastle University – UK
peter.davison@newcastle.ac.uk

## ABSTRACT

*The aim of this paper, is to provide a day-ahead optimal scheduling scheme for a multi-energy microgrid (MEM) which represents a real-world multi-vector demonstrator. The optimal scheduling scheme is tested against data from the multi-vector demonstrator in five different scenarios of the day-ahead demand and market prices. The assets of the multi-vector demonstrator include: a combined heat and power (CHP) plant, a central gas boiler, an energy storage system (ESS), a solar PV, an electric heater, and an electric vehicle (EV) filling station. The optimal scheduling scheme has been formed in order to capture the energy flows of the MEM. The problem is mathematically formulated as a mixed integer linear programming problem. A numerical case study verifies the effectiveness of the proposed scheduling scheme.*

## INTRODUCTION

Multi-Energy Systems (MES) are systems which can operate using multiple energy vectors or carriers (electricity, heating, transport etc.). Operating an energy system as such offers economic, technical, as well as environmental benefits [1]. Microgrids which operate in order to serve more than one energy vector are often referred to as Multi-Energy Microgrids (MEMs). The optimal scheduling of multi-energy microgrids aims to minimize the microgrid operational cost [2] in order to satisfy local multi-energy loads (e.g. electrical and heating loads), utilising dispatchable and non-dispatchable local energy sources, and import/export power from/to the power grid, during a certain time period (which is usually 24 hours).

A wide range of studies have been conducted for optimally scheduling a microgrid. Different scheduling methods have been proposed by individual platforms as well as independent research, more references of which can be found at [2]. The majority of MEM scheduling studies consider multi-energy microgrids with assets which operate centrally and serve aggregated electrical and aggregated heating loads, as the study presented in [3], where a robust energy management scheme for a MEM is proposed. Very few MEM scheduling studies take into account the individual assets of microgrid loads. The study presented in [4], proposes a receding horizon corrective scheduling model for MEMs, where individual household assets are taken into account. However, electric and heating energy generation from the central units towards each load (i.e. energy flow) is not captured in this study.

In this paper, we propose a day-ahead optimal scheduling scheme for a MEM. The scheduling scheme is formulated according to the topology of the real-world multi-vector demonstrator illustrated in Figure I. Multi-vector demonstrators represent multi-energy systems in their actual operating conditions (e.g. a university campus). The multi-vector demonstrator under study is a representation of the present and future assets of Newcastle Helix, which is situated in the North East of England [5]. The multi-vector demonstrator is composed of three buildings. Buildings B1 and B3 represent an educational and an office building respectively. Building B2 represents a very small office space. MEM components include a CHP plant which imports gas from the natural gas network and is connected to the three buildings through electricity and district heating networks, a central gas boiler which also imports gas from the natural gas network, an ESS and a solar PV allocated in the ground floor and roof (respectively) of building B1, an electric heater allocated in building B2, and an EV filling station. The consideration of the individual assets of the MEM loads enables the proposed optimal scheduling scheme to also capture the electricity and heating produced for each building from the CHP, main grid and gas boiler (i.e. the energy flows within the microgrid). The proposed method is tested against metered data from the demonstrator in five different scenarios of the day-ahead demand and market prices.

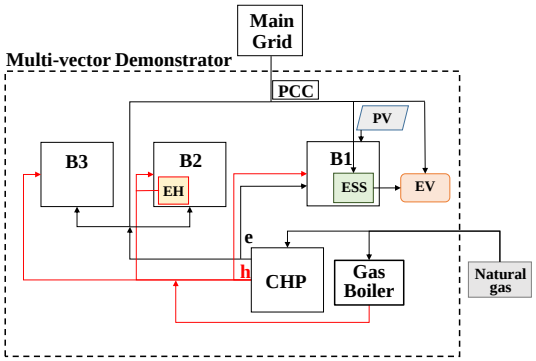


*Figure I. The Multi-vector demonstrator under study.*

Microgrid components are modelled as linear functions, which provides computational efficiency and model scalability. The problem is mathematically formulated as a mixed-integer linear programming problem (MILP). The scheduling horizon is 24 hours with half-hourly dispatch intervals (i.e. 48 time intervals). The rest of this paper is structured as follows. Firstly, component modelling is presented. Secondly, the mathematical representation of the optimal scheduling is formed. Thirdly, a numerical case study is presented, and finally the paper closes with conclusions and future work.

## MEM ASSET MODELLING

In this paper, it is considered that the microgrid operator is responsible for the operation of the MEM and all components are centrally controlled. The microgrid imports/exports power from/to the main grid through the point of common coupling (PCC). Modelling of the CHP, connection to the main grid, ESS, EV Filling Station, Gas Boiler, Electric Heater and Solar PV are presented below.

### Combined Heat and Power plant

The multi-energy microgrid is equipped with a central Combined Heat and Power plant. Power and heat production is considered to be coupled. Electricity produced is distributed to the loads through the MEM electric network. Heating produced is distributed through the district heating network of the MEM. The CHP is modelled through equations (1) – (9) as follows.

$$P^t_{CHP} = \eta^e_h H^t_{CHP}\ ,\ \forall t\in\Omega_T=\{1\dots48\} \quad (1)$$

$$\sum_{i=1}^{3} p^{B_i,\,t}_{CHP} + P^t_{Sell} = P^t_{CHP},\ \forall t\in\Omega_T \quad (2)$$

$$\sum_{i=1}^{3} h^{B_i,\,t}_{CHP} = H^t_{CHP}\ ,\ \forall t\in\Omega_T \quad (3)$$

$$p^{B_i,\,t}_{CHP},\ h^{B_i,\,t}_{CHP} \geq 0,\ \ \forall t\in\Omega_T,\ i=\{1,2,3\} \quad (4)$$

$$P^{Min}_{CHP} u^t_{CHP} \leq P^t_{CHP} \leq P^{Max}_{CHP} u^t_{CHP},\ \forall t\in\Omega_T \quad (5)$$

$$u^t_{CHP} - u^{t-1}_{CHP} \geq SU^t_{CHP}\ ,\ \forall t\in\Omega_T, SD^t_{CHP}, u^t_{CHP}\in\{0,1\} \quad (6)$$

$$u^{t-1}_{CHP} - u^t_{CHP} \geq SD^t_{CHP}\ ,\ \forall t\in\Omega_T,\ SU^t_{CHP}, u^t_{CHP}\in\{0,1\} \quad (7)$$

$$P^t_{CHP} - P^{t-1}_{CHP} \leq RU_{CHP}\ ,\ \ \forall t\in\Omega_T \quad (8)$$

$$P^{t-1}_{CHP} - P^t_{CHP} \leq RD_{CHP}\ ,\ \ \forall t\in\Omega_T \quad (9)$$

Where, (1) describes the power $P^t_{CHP}$ and heat $H^t_{CHP}$ output of the CHP with $\eta^e_h$ electric to heat ratio, (2) calculates the power produced for each building $p^{B_i,\,t}_{CHP}$ and the power $P^t_{Sell}$ sold to the main grid at each time interval, (3) calculates the heat $h^{B_i,\,t}_{CHP}$ produced for each building at each time interval, (4) ensures the positiveness of $p^{B_i,\,t}_{CHP}$ and $h^{B_i,\,t}_{CHP}$, (5) sets the limits of the output power, (6)-(7) and (8)-(9) are start-up/shut-down and ramp-up/down constraints respectively.

### Main grid connection

Main grid connection is expressed through equations (10)-(15).

$$P^t_{grid} = P^t_{Buy} - P^t_{Sell},\ \forall t\in\Omega_T \quad (10)$$

$$P^t_{Buy} = \sum_{i=1}^{3} p^{B_i,\,t}_{grid} + P^t_{gridESS} + P^t_{gridEV},\ \forall t\in\Omega_T \quad (11)$$

$$0 \leq P^t_{Buy} \leq x^t \cdot M\ ,\ \ \forall t\in\Omega_T \quad (12)$$

$$0 \leq P^t_{Sell} \leq y^t \cdot \mu\ ,\ \ \forall t\in\Omega_T \quad (13)$$

$$P^{b,t}_{grid},\ P^t_{gridESS},\ P^t_{gridEV} \geq 0,\ \ \forall t\in\Omega_T \quad (14)$$

$$x^t + y^t \leq 1,\ \ \forall t\in\Omega_T,\ x^t, y^t\in\{0,1\} \quad (15)$$

Where (10) expresses the main grid power at each time interval, with $P^t_{Buy}$ power bought and $P^t_{Sell}$ power sold from the CHP (used in equation (2)), (11) calculates the power bought from the main grid for each building, the ESS and the EV filling station, (12)-(13) set the limits for the power bought and sold from/to the main grid respectively, (14) ensures the positiveness of the variables $P^{b,t}_{grid}$, $P^t_{gridESS}$ and $P^t_{gridEV}$, and (15) ensures that power is not bought and sold at the same time interval. The number $\mu$ sets the upper limit of exported power and $M$ represents a very large number.

### Energy Storage System

An energy storage system (ESS) is located in building B1. The ESS is charged from the main grid and discharged in order to feed the EV filling station. It is modelled using the following set of equations.

$$C^{t-1} = C^t + \left(\frac{Pdch^t}{\eta} - \eta Pch^t\right)\Delta\tau\ ,\ \forall t\in\Omega_T \quad (16)$$

$$C^{Min} \leq C^t \leq C^{Max}\ ,\ \forall t\in\Omega_T \quad (17)$$

$$u^t \cdot Pch^{Min} \leq Pch^t \leq u^t \cdot Pch^{Max}\ ,\ \forall t\in\Omega_T \quad (18)$$

$$v^t \cdot Pdch^{Min} \leq Pdch^t \leq v^t \cdot Pdch^{Max}\ ,\ \forall t\in\Omega_T \quad (19)$$

$$u^t + v^t \leq 1,\ u^t, v^t\in\{0,1\} \quad (20)$$

Where, (16) describes the energy balance equation of the ESS with $C^t$ capacity, $\eta$ battery charging/discharging efficiency and $Pch^t_s/Pdch^t_s$ charging/discharging power, (17) sets the ESS capacity limits, (18)-(19) describe the power charging and discharging limitations of the ESS, and (20) expresses the ability of the ESS to either charge or discharge at each time interval $t$.

### Electric Vehicle Filling Station

The EV filling station is fed by the ESS and main grid. It is modelled as a Li-ion battery which charges during a forecasted time period, through equations (21)-(26) according to [6] as follows:

$$SOC^t = SOC^{t-1} u^{t-1}_{EV} + \frac{\eta^{charg}}{E^{Max}_{EV}} E^{t-1}_{EV}\,\Delta\tau\ ,\ \forall t\in\Omega_T \quad (21)$$

$$0 \leq P^t_{EV} \leq u^t_{EV}\, P^{Max}_{EV} \frac{1-SOC^t}{1-SOC^{CC,CV}},\ \forall t\in\Omega_T \quad (22)$$

$$0 \le P_{EV}^{t} \le u_{EV}^{t} \cdot P_{EV}^{Max}, \forall t \in \Omega_T \quad (23)$$

$$SOC_{Min} \le SOC^{t} \le SOC_{Max}, \forall t \in \Omega_T \quad (24)$$

$$SOC^{t=tarr} = SOC_{Arr} \quad (25)$$

$$SOC^{t=tdep} = SOC_{Dept} \quad (26)$$

Where (21) expresses the state of charge $SOC^t$ of the EV battery according to $u_{EV}^t$ which indicates the existence of a car (0/1) at each time interval, (22) and (23) set the upper and lower limits for the EV battery power and derive from the assumption that the EV battery charging method is the CC,CV method for Li-ion batteries (the interesting reader can refer to [6]), (24) describes the minimum and maximum allowable state of charge limits, (25) and (26) describe the EV filling station initial state of charge at the time of arrival and the EV filling station target state of charge at the time of departure respectively.

## Gas Boiler

To provide operational flexibility, CHPs are often operated in coordination with a gas boiler. We have considered a central gas boiler with maximum output 500kW$_{th}$ and efficiency $eff_{boil}$=0.9, through equations (27)-(28).

$$H_{boil}^{t} = eff_{boil} \cdot F_{boil}^{t} = \sum_{i=1}^{3} h_{boil}^{B_i\, t}, \forall t \in \Omega_T \quad (27)$$

$$0 \le H_{boil}^{t} \le H_{boil}^{Max}, \forall t \in \Omega_T \quad (28)$$

## Electric Heater

Building B2 consists of a small office space. This building apart from the CHP is also heated by an electric heater. It is assumed that the heater operates during office hours (9:00AM-17:30PM), with a 2 kW$_{th}$ output.

## Solar PV

A PV panel is located on the roof of building B1. An example of the metered PV output is presented in Figure II. The presented dataset is also used for the numerical simulations presented in this paper.

## MATHEMATICAL FORMULATION

The proposed optimal scheduling of the multi-vector demonstrator is formulated as a mixed integer linear programming problem. The main aim of the proposed method is to minimize the operational cost of the multi-energy microgrid. Operational costs include: costs due to power imported/exported from/to the distribution network, the CHP cost function, start-up/shut-down costs of the CHP, and the gas boiler cost function.

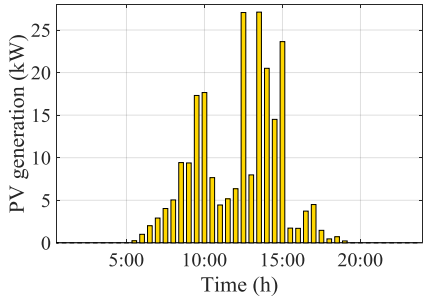


*Figure II. Metered solar PV generation of building B1.*

Minimize

$$\sum_{t=1}^{T=48} \left\{ \begin{array}{c} c_{grid}^{t} P_{grid}^{t} + \\ \left(\alpha_{CHP} P_{CHP}^{t} + \beta_{CHP}\, u_{CHP}^{t}\right) + \\ \left(c_{SU} SU_{CHP}^{t} + c_{SD} SD_{CHP}^{t}\right) + \\ c_{boil} H_{boil}^{t} \end{array} \right\} \quad (29)$$

Subject to constraints (1)–(28), and:

$$Ed_{B1}^{t} - PV^{t} = p_{grid}^{B1,t} + p_{CHP}^{B1,\,t}, \forall t \in \Omega_T \quad (30)$$

$$Ed_{b}^{t} = p_{grid}^{b,t} + p_{CHP}^{b,\,t}, \forall t \in \Omega_T, \forall b \in \{B2, B3\} \quad (31)$$

$$P_{EV}^{t} = Pdch^{t} + p_{grid}^{EV,\,t}, \forall t \in \Omega_T \quad (32)$$

$$h_{CHP}^{B_i,\,t} + h_{boil}^{B_i\,t} \ge H_{d}^{B_i,\,t}, \forall t \in \Omega_T, \forall i \in \{1,3\} \quad (33)$$

$$h_{CHP}^{B2,\,t} + h_{boil}^{B2\,t} \ge H_{d}^{B2,\,t} - EH^{B2,\,t}, \forall t \in \Omega_T \quad (34)$$

Where (30)-(31) describe the electric energy balance for each building (*B1*, *B2*, *B3)*, (32) describes the electric energy balance for the EV filling station, and (33)-(34) express the heating energy balance in order to satisfy the forecasted heating demand of buildings B1, B2 and B3.

## NUMERICAL SIMULATIONS

To test the proposed scheduling scheme of the multi-vector demonstrator, a numerical case study is presented. Available real-world metered data from the multi-vector demonstrator are used for the simulations. Estimated data are used for the future assets and the non-metered points of the multi-vector demonstrator. Electrical demand is represented by actual metering points from Newcastle Helix and is presented in Figure III and Figure IV. Heating demand is estimated according to the actual calculated annual heating demand of 2018 (kWh/m$^2$/year) of building B1 and appropriately scaled according to the building area (m$^2$) of buildings B2 and B3, as shown in Figure VI. The CHP is assumed to have 0.76 power/heat ratio and technical characteristics presented in Table I which have been appropriately scaled based on [7]. Data for the Energy Storage System of building B1 are presented in Table II. As very few electric vehicles currently circulate this area, it is assumed that two EVs arrive during the 24-hour scheduling horizon, i.e. at 8:30AM, 12:30PM and depart at 12:00PM, 15:00PM respectively. Data for the EV batteries are presented in Table II. Half-hourly market prices extracted from Elexon are presented in Figure V. Gas boiler price is set equal to 0.0238£/kWh.

*Table I. CHP Characteristics.*

| $\alpha_{CHP}$ (£/kWh) | $\beta_{CHP}$ (£) | $c_{SU}$ (£) | $c_{SD}$ (£) | $P_{CHP}^{Min}$ *(kW)* | $P_{CHP}^{Max}$ *(kW)* |
|---|---|---|---|---|---|
| 0.28 | 40 | 24 | 24 | 100 | 1000 |

*Table II. ESS Data.*

| $CMax_s$ (kWh) | $PchMax_s$ (kW) | $PdchMax_s$ (kW) | $\eta_s$ |
|---|---|---|---|
| 100 | 50 | 50 | 90% |

*Table III. EV filling station Data [6, 8].*

| $P_{EV}^{Max}$ (kW) | $E_{EV}^{Max}$ (kWh) | $SOC^{CC,CV}$ | $SOCMin$ | $SOCMax$ |
|---|---|---|---|---|
| 6.6 | 30 | 85% | 30% | 80% |

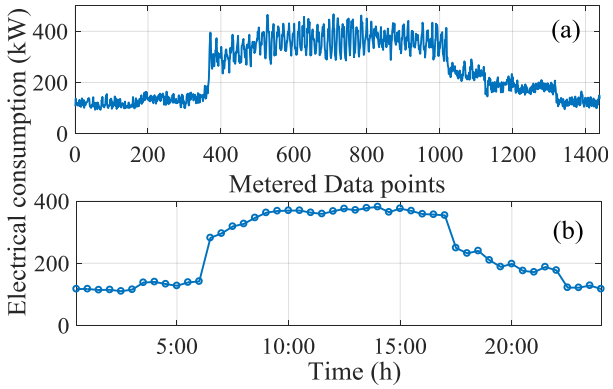


*Figure III. Electrical demand of building B1. (a) Metered data points, (b) Calculated half-hourly data.*

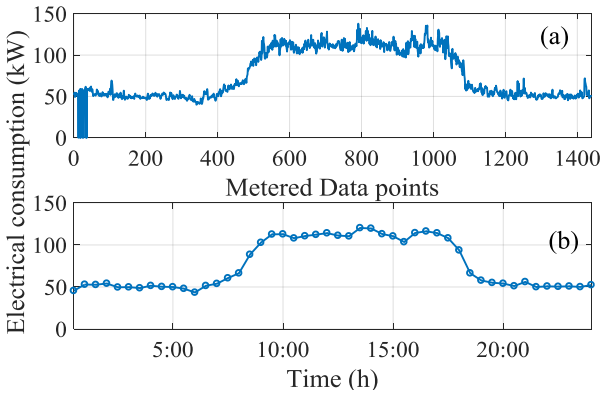


*Figure IV. Electrical demand of buildings B2 and B3 (summed, as metered). (a) Metered data points, (b) Calculated half-hourly data.*

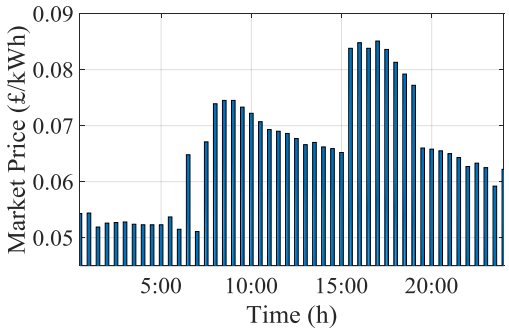


*Figure V. Day-ahead market prices*

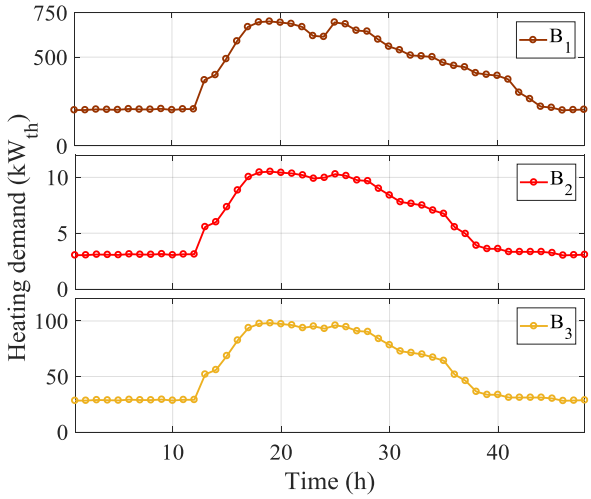


*Figure VI. Heating demand of buildings B1, B2, B3.*

## Simulation Results & Discussion

In this section, a numerical case study is presented. The simulations were run on a desktop computer, using IBM ILOG CPLEX v12.8 [9]. Five different scenarios for the day-ahead scheduling were tested. A reference scenario is created composed of the metered data and estimated data presented above. The other four scenarios have a ±5% and ±10% difference with respect to the reference scenario in the values of the electrical & heating demand, and market prices. The scenarios are presented in Table IV. The ESS capacity and EV SOC for all simulated scenarios are presented in Figure VII. The EV filling station is fed only by the ESS, which explains the same $SOC_{EV}$ value for all scenarios. In the figures below, it is shown that there is a straight analogue between the electric demand and the imported power, and the heating demand and the boiler output during the times that the CHP is turned off. This analogue is converted to an interdependency between the electric and heating energy vectors when the CHP is in operation as shown in the figures below. Furthermore, in Figure VIII, we observe that regardless the minor changes in the input values, there is almost a 50% difference in the CHP output between scenarios 3 and 4. The power imported from the main grid also has around 50% difference between scenarios 2 and 4. The gas boiler output has less alterations (around ±10%) with respect to the reference scenario (Figure X). Energy flow results have been used to calculate the total scheduled 24-hour generation from the CHP, main grid and gas boiler of the multi-vector demonstrator, as presented in Figure XI.

*Table IV. Simulated scenarios.*

| Scenario | Market Price | Electrical Demand | Heating Demand |
|---|---|---|---|
| 1 | +10% | -5% | -5% |
| 2 | -5% | -10% | +5% |
| 3 | +5% | +5% | +10% |
| 4 | +5% | +10% | -10% |

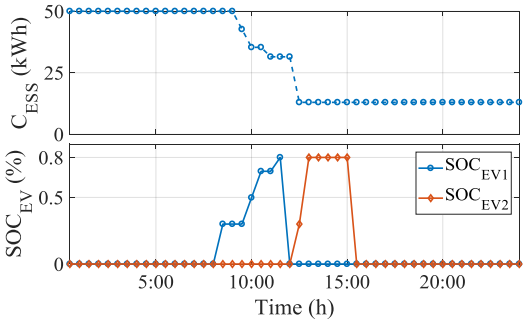


*Figure VII. (a) ESS Capacity, and (b) EV SOC (%)*

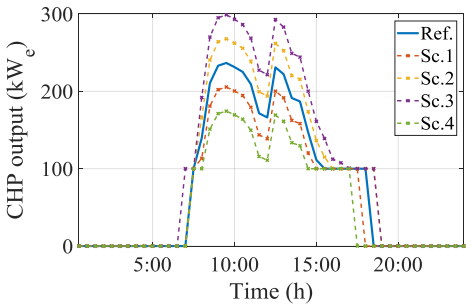


*Figure VIII. Scheduled CHP output for each scenario.*

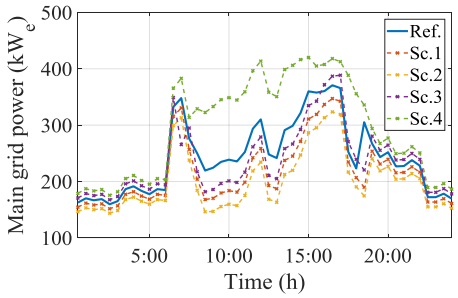


*Figure IX. Scheduled imported power for each scenario.*

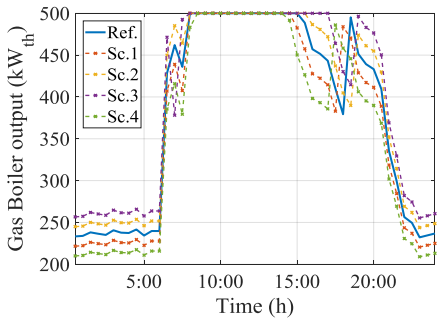


*Figure X. Scheduled Boiler Output for each scenario.*

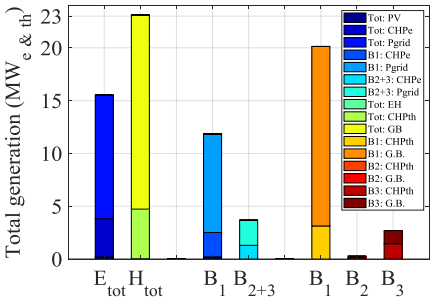


*Figure XI. Day-ahead generation: for total MEM and for each load (calculated from the hourly energy flows).*

## CONCLUSIONS

A scheduling scheme for a MEM which represents a multi-vector demonstrator is presented. The problem is mathematically formulated as a MILP problem. Five different scenarios for the values of the day-ahead electric demand, heating demand and market prices are tested. The results show firstly, the interdependency between the multi-energy vectors of the MEM, secondly, an application of actual metered data of a multi-vector demonstrator, and thirdly the effectiveness of the proposed scheduling scheme. The 50% difference between scenarios 2-4 in the CHP output and imported power for a small change of ±10% in the values of the simulated scenarios paves the way for our future work, which aims to include forecasting uncertainty in the optimal scheduling scheme of the multi-vector demonstrator.

## REFERENCES

[1] P. Mancarella, 2014, "MES (multi-energy systems): An overview of concepts and evaluation models," *Energy*, vol. 65, 1-17.

[2] S. Parhizi, H. Lotfi, A. Khodaei, S. Bahramirad, 2015, "State of the Art in Research on Microgrids: A Review," *IEEE Access*, vol. 3, 890 - 925.

[3] Y. Guo, C. Zhao, 2018, "Islanding-Aware Robust Energy Management for Microgrids," *IEEE Transactions on Smart Grid*, vol. 9, no. 2, 1301-1309.

[4] N. Holjevac, T.Capuder, N. Zhang, I. Kuzle, C. Kang, 2017, "Corrective receding horizon scheduling of flexible distributed multi-energy microgrids," *Applied Energy*, no. 207, 176-194.

[5] "Newcastle Helix," https://newcastlehelix.com/.

[6] S. I. Vagropoulos, A. G. Bakirtzis, 2013, "Optimal Bidding Strategy for Electric Vehicle Aggregators in Electricity Markets," *IEEE Transactions on Power Systems*, vol. 28, no. 4, 4031-4041.

[7] S. X. Chen, H. B. Gooi, 2012, M. Q. Wang, "Sizing of Energy Storage for Microgrids," *IEEE Transactions on Smart Grid* vol. 3, no. 1, 142-151.

[8] A. Hoke, A. Brissette, K. Smith, A. Pratt, D. Maksimovic, 2014, "Accounting for Lithium-Ion Battery Degradation in Electric Vehicle Charging Optimization," *IEEE Journal of Emerging and Selected Topics in Power Electronics*, vol. 2, no. 3, 691-700.

[9] "IBM ILOG CPLEX Optimization Studio," https://www.ibm.com/products/ilog-cplex-optimization-studio.